Electron Spin Resonance and Electron Spin Echo Modulation Spectroscopic Studies of Chromium Ion Location and Adsorbate Interactions in Calcined CrAPSO-11

Zhidong Zhu, Tomasz Wasowicz, and Larry Kevan*

Department of Chemistry, University of Houston, Houston, Texas 77204-5641

Received: March 3, 1997; In Final Form: September 12, 1997[⊗]

The local environment of the chromium ion in calcined CrAPSO-11, which may involve framework sites, is compared with the Cr ion environment in solid-state ion-exchanged (S)Cr−SAPO-11 which involves ion exchange into nonframework sites at high temperature. Powder X-ray diffraction confirms that CrAPSO-11 has the SAPO-11 framework and is highly crystalline. The ^{27}Al and ^{29}Si magic-angle-spinning nuclear magnetic resonance spectra are similar to those of corresponding SAPO-11 showing only one type of tetrahedral atom. As-synthesized CrAPSO-11 shows an ESR spectrum assignable to Cr(III), but on calcination this converts to Cr(V). (S)Cr−SAPO-11 forms Cr(V) directly since solid-state ion exchange occurs at high temperature. The UV−vis spectrum of calcined, hydrated CrAPSO-11 is assigned to Cr(V), and after dehydration the coordination for Cr(V) seems consistent with tetrahedral as expected for a framework site. Electron spin resonance (ESR) of calcined, hydrated CrAPSO-11 shows Cr(V) which is consistent with square-pyramidal coordination which gradually converts to Cr(V) in distorted tetrahedral coordination upon dehydration by heating in vacuum. The ESR spectrum of ion-exchanged (S)Cr−SAPO-11 shows Cr(V), but it does not convert to tetrahedral coordination upon heating in vacuum. Hydrogen reduction shows that Cr(V) in (S)-Cr−SAPO-11 can be reduced to a several hundred gauss broad ESR signal assignable to Cr(III). Reduction by H_2 of calcined CrAPSO-11 does not produce Cr(III) observable by ESR. The interactions between Cr(V) in calcined CrAPSO-11 and (S)Cr−SAPO-11 with D_2O, CH_3OD, CD_3OH, ND_3, and pyridine adsorbates are also compared. Differences in the kinetics of absorbate coordination between calcined CrAPSO-11 and (S)-Cr−APSO-11 are observed. All these differences support different Cr(V) sites in these two materials. ^{31}P electron spin echo modulation of CrAPSO-11 shows that Cr(V) is surrounded by about 11−12 phosphorus nuclei at 0.58 nm, which is consistent with Cr(V) in CrAPSO-11 being in a framework phosphorus position.

Introduction

Microporous silicoaluminophosphate (SAPO) molecular sieves have been reported with various framework-substituted transition-metal ions.[1−5] These are potential catalytic materials of interest. In particular, framework-substituted materials may have stability or catalytic advantages over ion-exchanged materials. Chromium-incorporated microporous aluminophosphates are active, selective, and recyclable catalysts for the oxidation of benzylic and cyclic alcohols with oxygen or *tert*-butyl hydroperoxide as oxidants.[6] The possibility of chromium ion substitution into aluminophosphate (AlPO) and silicoaluminophosphate (SAPO) frameworks has been studied.[7−10] Some results suggest that chromium ion cannot be incorporated into the framework of SAPO-34 and AlPO-5.[7,8] Other results are interpreted as evidence for chromium ion substitution in a framework position in AlPO-11.[9] It has also been suggested that chromium ion can be incorporated into the framework of SAPO-11 by comparing the behavior of CrAPSO-11 with that of MAPSO-11 (M = Mg, Zn, Mn, Fe, and Ni).[10]

Electron spin resonance (ESR) and electron spin echo modulation (ESEM) have been found to be powerful methods for studying the location of transition-metal ions in molecular sieves.[11] In this investigation, we use ESR and ESEM together with UV−vis spectroscopy to show chromium ion incorporation into the framework of SAPO-11. Cr(III) is initially incorporated, but Cr(V) is produced after calcination and is the valence state studied here. Cr(V) is incorporated into the framework of SAPO-11 in phosphorus sites.

Experimental Section

Synthesis and Sample Treatment. SAPO-11 was synthesized according to the literature.[12] CrAPSO-11 was hydrothermally synthesized according to the following general procedure.[4,13] A solution was prepared by stirring 9.13 mL of 85 wt % H_3PO_4 and 40 mL of water for 10 min. Then 9.21 g of Catapal B alumina was added gradually to this solution, which was stirred for 2 h. Subsequently, 0.99 g of 40 wt % LUDOX HS (silica) and 3.4 mL of water were added dropwise with stirring for about 30 min. To this solution, 4 mL of 1.69×10^{-2} M $CrCl_3$ was added dropwise and stirred for 2 h. Finally, 9.26 mL of diisopropylamine was added. The solution was aged with stirring at room temperature for 24 h to form a homogeneous gel. The reaction mixture was placed in a stainless steel pressure vessel lined with Teflon and heated in an oven at 220 °C at autogenous pressure for 4 days. The product was collected by filtration, washed, and dried in air at 110 °C overnight. As-synthesized CrAPSO-11 was then calcined for 18 h at 600 °C in flowing oxygen in order to remove the diisopropylamine template. Calcined CrAPSO-11 is cooled in air and becomes hydrated by exposure to moisture in the air. Thus, the calcined material is described as calcined, hydrated CrAPSO-11. The chemical composition of calcined, dehydrated CrAPSO-11 is $H_{0.038}(Cr_{0.002}Si_{0.018}Al_{0.510}P_{0.470})\ O_2$, which corresponds to 0.17 wt % Cr based on electron microprobe analysis in vacuum.

Calcined CrAPSO-11 contains paramagnetic Cr(V) and possibly extraframework Cr(VI) [see below]. To test for extraframework Cr(VI), 1 g of calcined CrAPSO-11 was stirred in 20 mL of 1 M $Ca(NO_3)_2$ solution for 14 h. The filtrate was collected, and 1 M $AgNO_3$ was added dropwise to test for

[⊗] Abstract published in *Advance ACS Abstracts,* December 1, 1997.

S1089-5647(97)00787-6 CCC: $14.00

CrO_4^{2-} [i.e., Cr(VI)], but no Ag_2CrO_4 precipitate was formed. It is concluded that extraframework Cr(VI) is not detectable in calcined CrAPSO-11.

Chromium ion was ion-exchanged into H−SAPO-11 by high-temperature solid-state method. It has been shown that such a solid-state method incorporates metal ions into the same ion-exchange sites as introduced by liquid-phase ion exchange and that these are extraframework sites.[14,15] $CrCl_3 \cdot 6H_2O$ (0.01 g) was ground with 1 g of H−SAPO-11 in a mortar until the powder looked homogeneous. The solid mixture was pressed in a stainless steel die with a force of 2 tons to prepare a pellet of 12 mm in diameter and 3 mm thickness. The pellet was then broken into small chunks, placed in a quartz boat, and heated in a furnace in flowing oxygen at 600 °C for 21 h. The reaction product was cooled slowly in air to room temperature and ground to a fine powder. This product is termed (S)Cr−SAPO-11. Since the solid-state ion-exchange procedure involves heating to 600 °C, the product is comparable to *calcined*, hydrated CrAPSO-11 and contains Cr(V) instead of Cr(III) as shown below.

To study the interaction of calcined CrAPSO-11 and (S)Cr−SAPO-11 with adsorbates, samples were prepared according to the following general procedure. About 10 mg of calcined, hydrated CrAPSO-11 was evacuated at 350 °C for 18 h to remove adsorbed water, and then it was exposed to an adsorbate at its room-temperature vapor pressure for liquids or at a pressure of about 360 Torr for gases. The following adsorbates were used: D_2O, CH_3OD, CD_3OH, ND_3, and C_5D_5N (Aldrich Chemicals, 99 atom % D).

Measurements. The synthetic molecular sieves were examined by powder X-ray diffraction (XRD) on a Philips PW 1840 diffractometer. Both SAPO-11 and CrAPSO-11 were investigated by thermogravimetric analysis (TGA) on a Dupont 2100 thermal analyzer at a rate of 10 °C/min in flowing oxygen. Diffuse reflectance ultraviolet−visible (UV−vis) spectra were measured with a Perkin-Elmer 330 spectrophotometer equipped with a 60 mm Hitachi integrating sphere accessory. Powder samples were loaded in a quartz cell with Suprasil windows, and spectra were collected in the 200−800 nm wavelength range against an Al_2O_3 standard. Infrared spectra were obtained with a Nicolet 740 FTIR spectrophotometer by the KBr pellet method. NMR experiments were performed on a Bruker 400 MHz spectrometer. X-band ESR spectra were recorded at 77 K with a Bruker ESP 300 ESR spectrometer. ESEM spectra were recorded at 4 K with a Bruker ESP 380 pulsed FT-ESR spectrometer. Three-pulse echoes were recorded with a $\pi/2-\tau-\pi/2-T-\pi/2$ pulse sequence as a function of T. The value of τ in the three-pulse experiment was optimized to suppress one unwanted modulation.[16,17] Echo modulation patterns were simulated using a point-dipole spherical approximation. The number of interacting nuclei N, the distance R, and the isotropic hyperfine coupling A_{iso} were determined by fitting simulations to experimental data.[16,17]

Results

X-ray Powder Diffraction. The structures of as-synthesized and calcined CrAPSO-11 and H−SAPO-11 show no significant differences in their XRD patterns and agree with the literature data for SAPO-11.[5] A good baseline confirms good crystallinity for synthesized CrAPSO-11. The XRD data also do not show any $CrPO_4$ phase or Cr_2O_3 phase.

TGA. The TGA curves of as-synthesized SAPO-11 and CrAPSO-11 show three stages of weight loss at ∼70, ∼280, and ∼370 °C. The first stage of weight loss is assigned to the desorption of physically adsorbed water. The weight loss near 280 °C is assigned to physically adsorbed diisopropylamine, and the weight loss near 370 °C is assigned to protonated diisopropylamine which indicates the presence of acid sites. In CrAPSO-11 an additional weight loss near 470 °C is observed, indicating additional, stronger acid sites in comparison to SAPO-11. Stronger acid sites are expected if Cr(III) substitutes for framework P(V).

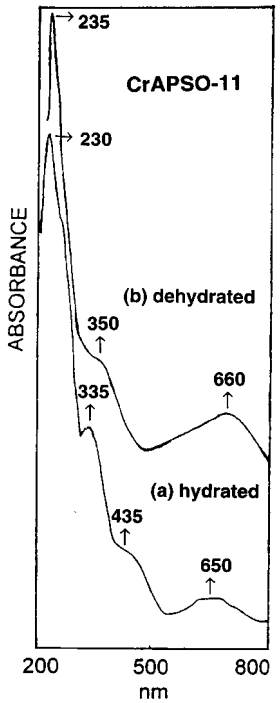

Figure 1. UV−vis spectra of (a) calcined, hydrated CrAPSO-11 and (b) calcined, dehydrated CrAPSO-11.

Infrared Spectra. There have been some suggestions of FTIR band shifts or new bands in the 1300−400 cm^{-1} range associated with metal ion framework substitution in microporous oxides.[9,18] However, we do not find significant differences between SAPO-11 and CrAPSO-11 in this FTIR region.

UV−vis Spectra. The spectra of calcined, hydrated CrAPSO-11, and calcined, dehydrated (550 °C for 14 h in vacuum) CrAPSO-11 are shown in Figure 1. In calcined, hydrated CrAPSO-11 four bands at 230, 335, 435, and 650 nm are observed, while in calcined, dehydrated CrAPSO-11 only three bands at 235, 350, and 660 nm are observed, and the 435 nm band seems to be absent. These higher bands (230−235 nm, 335−350 nm) have typically been assigned to charge-transfer transitions associated with Cr(VI);[8] however, we did not chemically detect Cr(VI) in our calcined samples. On the other hand, the ESR studies to be described below clearly show that Cr(V) is present in the calcined samples. Furthermore, d−d optical transitions of Cr(V) occur in the same spectral region.[19] Thus, we assign these optical bands to Cr(V). Cr(V) is formed by oxidation of Cr(III) during calcination. The three bands at 660, 350, and 235 nm in calcined, dehydrated CrAPSO-11 seem consistent with transitions for Cr(V) within the SAPO-11 framework in tetrahedral coordination.[20] Then the four bands in calcined, hydrated SAPO-11 can be assigned to Cr(V) in square-pyramidal or distorted octahedral coordination where the additional coordination is due to water. The Cr(V) assignment agrees with the ESR results given below.

MAS NMR. The ^{27}Al MAS NMR of calcined CrAPSO-11 consists of a single resonance at 35 ppm relative to hydrated aluminum nitrate which is assignable as tetrahedral ^{27}Al.[21] The MAS NMR spectrum of ^{29}Si in calcined CrAPSO-11 consists of an broad resonance at −90 to −112 ppm relative to

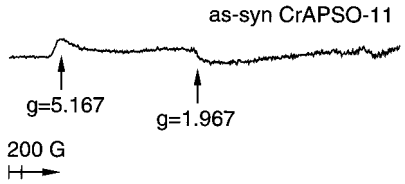

Figure 2. ESR spectrum at 77 K of as-synthesized CrAPSO-11.

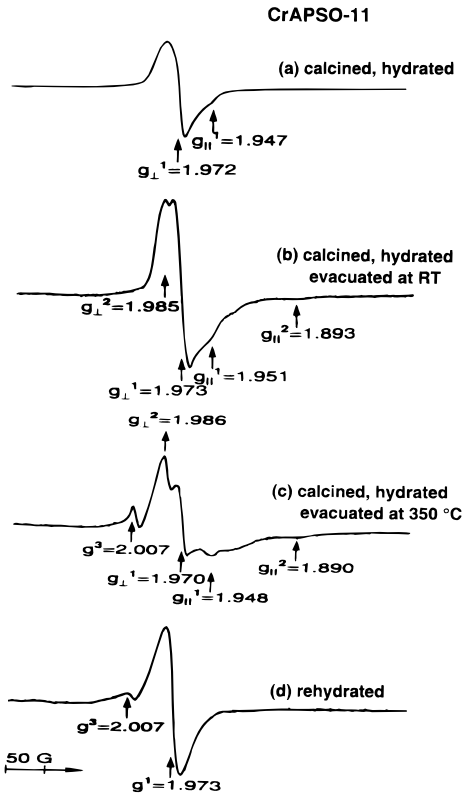

Figure 3. ESR spectra at 77 K of calcined CrAPSO-11: (a) hydrated, (b) after 20 h evacuation at room temperature; (c) after 18 h evacuation at 350 °C, and (d) after subsequently adsorbed D_2O.

tetramethylsilane which is similar to that of tetrahedral ^{29}Si in SAPO-11.[22] The broadness is consistent with the existence of Si islands.

ESR of CrAPSO-11. As-synthesized CrAPSO-11 shows the broad ESR spectrum in Figure 2 with a positive lobe at $g = 5.17$ and a broad line at $g = 1.97$. These two features have both been assigned separately to Cr(III) on silica,[23] alumina,[24] and chromosilicate catalysts.[25] In most preparations the line near $g = 2$ appears with varying intensity. The intensity of the positive lobe greatly varies with the sample preparation, and its position varies from $g \sim 5$ to $g \sim 4$. This low-field feature was originally interpreted as involving substantial D and E zero-field splittings.[24] A recent reanalysis of chromium ESR spectra in silica and alumina supports this.[26]

After calcination and hydration during cooling, CrAPSO-11 shows a much narrower ESR spectrum (Figure 3a) which can be clearly assigned to Cr(V),[27−29] possibly in square-pyramidal coordination.[27] Cr(V) is formed by oxidation of Cr(III) during calcination. According to the g formulas[30] for square-pyramidal geometry

$$g_\perp = g_e - 2\lambda/\Delta_0 \qquad g_\parallel = g_e - 8\lambda/\Delta_1$$

where λ is the spin−orbit coupling constant of 160 cm^{-1} for Cr(V) in an oxide environment[31] and Δ_0 and Δ_1 are two lowest energy UV transitions for calcined, hydrated CrAPSO-11; the calculated g values are $g_\perp = 1.981$ and $g_\parallel = 1.946$. These are in good agreement with the experimental values of $g_\perp = 1.972$ and $g_\parallel = 1.947$ (Figure 3a) which seems to support the assignments of the UV spectrum and the ESR spectrum to square-pyramidal Cr(V). If distorted octahedral geometry is assumed, $g_\perp < g_\parallel$, which does not agree with the experimental g parameters.

Figure 3 shows the changes in the ESR spectra at 77 K after treatment of calcined, hydrated CrAPSO-11 at various temperatures. Calcined, hydrated CrAPSO-11 shows only the paramagnetic species assigned to square-pyramidal Cr(V). A second Cr species with $g_\perp = 1.985$ and $g_\parallel = 1.893$ is observed after the sample is evacuated at room temperature for 20 h (Figure 3b). After this sample is further evacuated at 350 °C for 18 h, the second species becomes more prominent, and a third species is observed with $g^3 = 2.007$ (Figure 3c). After this sample is evacuated at 550 °C for 14 h, only the second and third paramagnetic species remain. After subsequent D_2O adsorption for 17 h at room temperature, Cr(V) species one is regenerated although the $g_\parallel$ anisotropy is not as clear as in the originally calcined, hydrated sample (Figure 3d).

The second signal with $g_\perp = 1.985$ and $g_\parallel = 1.893$ is typical of Cr(V) in distorted tetrahedral coordination.[28] From the g formulas for tetrahedral geometry[32] and the UV data for calcined, dehydrated CrAPSO-11 for the lowest transition energy,

$$g_\parallel = g_e - 8\lambda/\Delta_0 \qquad g_\perp = g_e - 2\lambda/\Delta_0$$

the calculated g values are $g_\perp = 1.981$ and $g_\parallel = 1.917$, which agree reasonably with the experimental values. This confirms the assignments of the UV and ESR data for dehydrated CrAPSO-11 to distorted tetrahedral Cr(V). It has been previously suggested that tetrahedral Cr(V) can rearrange to square-pyramidal Cr(V) under the influence of added ligands such as H_2O.[27]

After CrAPSO-11 is dehydrated at 350 °C, a signal at $g = 2.007$ is observed. A similar signal is also observed in dehydrated SAPO-11 and is attributed to lattice defects in SAPO-11.[33]

Figure 4 shows the change in ESR spectra during reduction of calcined, hydrated CrAPSO-11 by hydrogen. The sample was evacuated at room temperature followed by reduction by 760 Torr of hydrogen at 200 °C for 0.5 h. The ESR spectrum of the sample after this treatment shows square-pyramidal and tetrahedral Cr(V). After further reduction by hydrogen at 300 °C for 0.5 h, the lattice defect species with $g^3 = 2.007$ is produced. The behavior is thus similar to heating in vacuum. After further reduction to 400 °C for 0.5 h, a signal of O_2^- is produced with $g_1 = 2.021$, $g_2 = 2.009$, and $g_3 = 2.003$.[34] After reduction at 500 °C, the O_2^- signal largely dominates the ESR spectrum. This suggests that Cr(V) donates an electron to O_2 and is oxidized to Cr(VI) for which there is some precedent.[35] No ESR evidence for Cr(III) production is seen.

ESR of (S)Cr−SAPO-11. We now contrast the above results on CrAPSO-11 with analogous experiments on solid-state ion-exchanged (S)Cr−SAPO-11. Figure 5 shows a nearly isotropic signal at $g^1 = 1.973$ for (S)Cr−SAPO-11 which by analogy to CrAPSO-11 can be assigned to square-pyramidal Cr(V). Evacuation at 350 °C produces only a lattice defect at $g^3 = 2.006$ and does not produce tetrahedral Cr(V) in contrast to CrAPSO-11.

Figure 6 shows the ESR spectra of (S)Cr−SAPO-11 after static hydrogen reduction. After reduction at 200 °C only square-pyramidal Cr(V) is seen in contrast to CrAPSO-11. Reduction at 400 °C produces a new, very broad signal at $g^4 =$

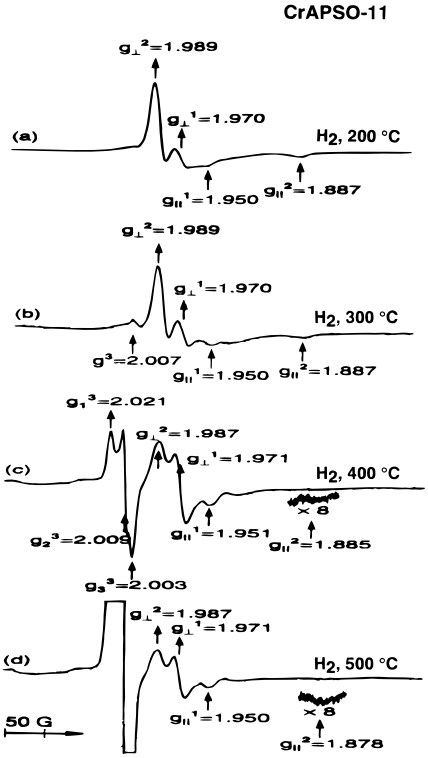

Figure 4. ESR spectra at 77 K of calcined, hydrated CrAPSO-11 reduced by 760 Torr of hydrogen for 0.5 h at (a) 200, (b) 300, (c) 400, and (d) 500 °C.

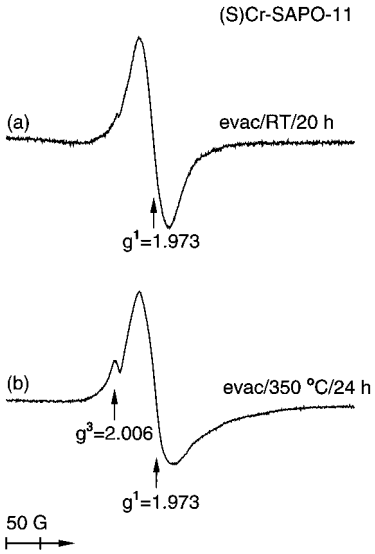

Figure 5. ESR spectra at 77 K of (S)Cr−SAPO-11: (a) after 20 h evacuation at room temperature and (b) after 24 h evacuation at 350 °C.

2.384 which can be assigned to Cr(III).[23−25] Further reduction at 500 °C completely converts the Cr(V) to Cr(III).

ESR of CrAPSO-11 and (S)Cr−SAPO-11 with Adsorbates. After calcined, hydrated CrAPSO-11 is dehydrated by evacuation at 350 °C, adsorption of D_2O vapor for 17 h regenerates square-pyramidal Cr(V) with little detectable g anisotropy (Figure 3d). Similar adsorption of CD_3OH generates the same ESR signal of Cr(V) with some g anisotropy. Adsorption of D_2O and CD_3OH for 17 h on dehydrated (S)-Cr−SAPO-11 also generates a nearly isotropic ESR signal of square-pyramidal Cr(V).

Figure 7 shows changes in the ESR spectra of CrAPSO-11 and (S)Cr−SAPO-11 dehydrated at 350 °C overnight with subsequently adsorbed ND_3. CrAPSO-11 initially shows Cr-

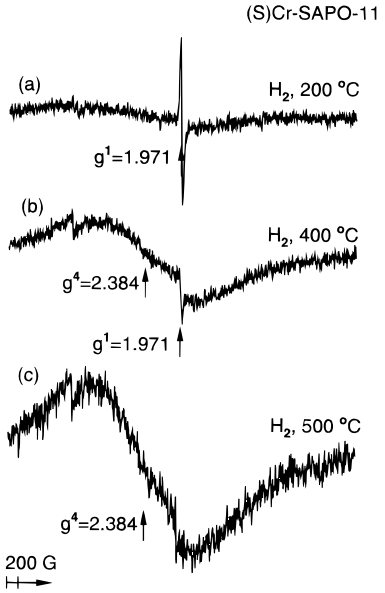

Figure 6. ESR spectra at 77 K of (S)Cr−SAPO-11 reduced by hydrogen for 0.5 h at (a) 200, (b) 400, and (c) 500 °C.

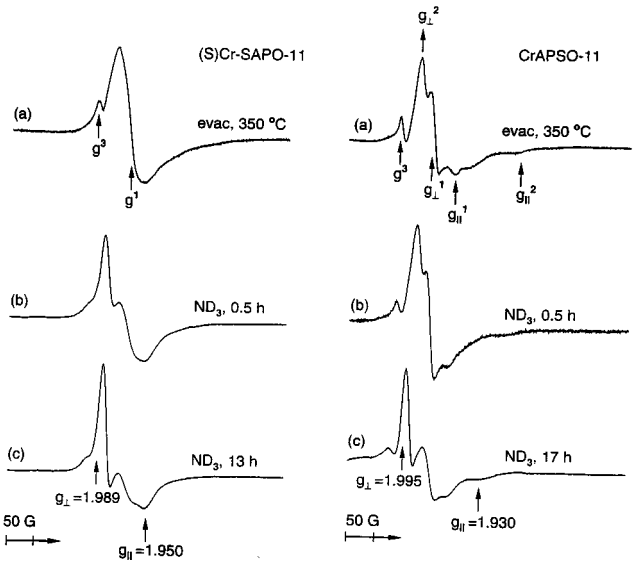

Figure 7. ESR spectra at 77 K of calcined, hydrated CrAPSO-11 and (S)Cr−SAPO-11 evacuated at 350 °C for 18 h with subsequently adsorbed ND_3 for 0.5 h and for 13/17 h.

(V) species 1 and 2 and a lattice defect (species 3). No change is seen for ND_3 adsorption for 0.5 h, but after 17 h Cr(V) species 2 seems to be replaced by a new ESR signal with $g_\perp = 1.995$ and $g_\parallel = 1.930$ while Cr(V) species 1 remains. It appears that tetrahedral Cr(V) species 2 forms a new complex with ND_3. (S)Cr−SAPO-11 reacts much more rapidly with ND_3 than does CrAPSO-11 and forms a new Cr(V) complex with ND_3 ($g_\perp = 1.989$ and $g_\parallel = 1.950$) in 0.5 h at the expense of Cr(V) species 1. The contrasting behaviors of CrAPSO-11 and (S)Cr−SAPO-11 again indicate different Cr(V) sites in these two materials.

The adsorption of pyridine for 13 h on (S)Cr−SAPO-11 dehydrated at 350 °C causes a broadening of Cr(V) species 1 and results in a new anisotropic signal (Figure 8). It seems probable that a new pyridine complex is formed with $g_\perp \sim g_1 = 1.973$ and $g_\parallel = 1.907$. The adsorption of pyridine by CrAPSO-11 for 13 h does not cause any change in its ESR spectrum which implies no significant interaction or complex formation.

Electron Spin Echo Modulation. ESEM experiments were done on calcined, dehydrated CrAPSO-11 and on (S)Cr−SAPO-

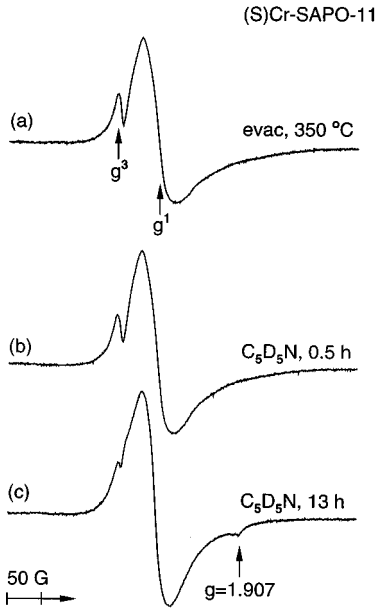

Figure 8. ESR spectra at 77 K of (S)Cr−SAPO-11 evacuated at 350 °C for 18 h with subsequently adsorbed C_5D_5N for 0.5 and 13 h.

TABLE 1: ESR Parameters at 77 K of Cr(V) in Calcined CrAPSO-11

treatment	$g_{\|\|}$	$g_{\perp}$	g_{iso}
calcined, hydrated	1.947	1.972	
evacuated at RT	1.951	1.973	
	1.893	1.985	
evacuated at 150 °C	1.948	1.970	
	1.890	1.986	
evacuated at 350 °C	1.948	1.970	
	1.890	1.986	
			2.007
$+D_2O$			1.976, 2.007
$+CH_3OD$			1.976, 2.007
$+ND_3$	1.930	1.995	
	1.947	1.972	

TABLE 2: ^{2}H ESEM Simulation Parameters for Cr(V) in Calcined CrAPSO-11 and (S)Cr−SAPO-11 with Various Adsorbates

sample	adsorbate	*N*	*R*, nm	A_{iso}, MHz
CrAPSO-11	D_2O	4	0.30	0.10
(S)Cr−SAPO-11	D_2O	4	0.33	0.06
CrAPSO-11	CH_3OD	2	0.32	0.12
(S)Cr−SAPO-11	CH_3OD	2	0.36	0.12
CrAPSO-11	CD_3OH	6	0.36	0.02
(S)Cr−SAPO-11	CD_3OH	6	0.38	0.10
CrAPSO-11	ND_3	6	0.34	0.04
(S)Cr−SAPO-11	ND_3	6	0.33	0.10

11 with various deuterated adsorbates. Table 2 summarizes the ESEM parameters. Analysis of the three-pulse ESEM spectrum of CrAPSO-11 hydrated with D_2O indicates that Cr(V) is coordinated to two water molecules situated at a Cr−D distance of 0.30 nm. The analogous simulation for (S)Cr−SAPO-11 hydrated with D_2O indicates that the Cr(V)−D distance is a little longer at 0.33 nm with two adsorbed molecules.

The ESEM data for CrAPSO-11 and for (S)Cr−SAPO-11 with adsorbed CH_3OD or CD_3OH indicates coordination to two methanols for both. Again the Cr(V)−D distances are a little greater for (S)Cr−SAPO-11.

The results for ND_3 adsorption show two coordinated molecules at similar distances to Cr(V) in both CrAPSO-11 and (S)Cr−APSO-11.

A three-pulse ^{31}P ESEM spectrum (Figure 9) was obtained for CrAPSO-11 evacuated at room temperature for 12 h. The

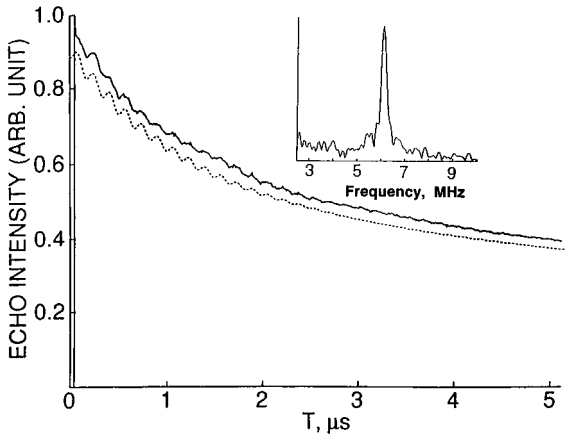

Figure 9. Experimental (—) and simulated (- - -) three-pulse ^{31}P ESEM spectra at 4 K of calcined, hydrated CrAPSO-11 evacuated at room temperature for 12 h.

spectrum is simulated with 11−12 phosphorus nuclei interacting with Cr(V) at a distance of 0.58 nm. The three-pulse ESE for (S)Cr−SAPO-11 does not show any ^{31}P modulation.

Discussion

Coordination and Location of Cr(V) in (S)Cr−SAPO-11. The formation of Cr(V) in microporous oxide materials by solid-state ion exchange at elevated temperature has been suggested for ZSM-5 and mordenite based on ESR data.[36] This is consistent with our assignment. More specifically, our ESR *g* values seem consistent with square-pyramidal Cr(V) coordinated to three oxygens of a six-ring in the large channel of SAPO-11 and to adsorbate ligands of water, methanol, and ammonia based on the ESEM data. Some distortion of square-pyramidal geometry would be necessary for this ligand arrangement. Such distortion seems to be supported by (a) the lack of ^{31}P modulation, indicating an offset position from the axis of a six-ring toward a Si-rich side, and by (b) somewhat longer than typical M^{x+}−D(adsorbate) distances (Table 2) of ∼0.28−0.30 nm for Cr(V) [0.049 nm radius] versus Cu(II) [0.073 nm radius].[15,37]

When (S)Cr−SAPO-11 is heated in vacuum to 350 °C (Figure 5) or in H_2 at 200 °C (Figure 6), the ESR spectrum of Cr(V) does not change. Thus, if weakly bound water ligands are lost, the possible change to trigonal coordination to three oxygens in a six-ring does not significantly change the ESR spectrum. It is significant that heating (S)Cr−SAPO-11 to 400 °C or above in H_2 does cause reduction of Cr(V) to Cr(III) based on the clear ESR spectral change. Thus, Cr(III) is stable in ion-exchanged Cr−SAPO-11.

Coordination and Location of Cr(V) in CrAPSO-11. The data show that Cr(V) in calcined CrAPSO-11, synthesized with $CrCl_3$ in the synthesis mixture, has numerous different characteristics from Cr(V) in ion-exchanged (S)Cr−SAPO-11. These significant differences clearly indicate quite different sites for Cr(V) in these two materials. The important question is whether Cr(V) in CrAPSO-11 is in a framework lattice site. Such a site should have tetrahedral symmetry unless there is additional coordination to an adsorbate. No evidence for tetrahedral Cr-(V) sites was found in (S)Cr−SAPO-11 as expected for an ion-exchange site.

Both the diffuse reflectance UV data and the ESR data for Cr(V) in CrAPSO-11 are consistent with square-pyramidal Cr-(V) in calcined, hydrated CrAPSO-11 which converts to tetrahedral Cr(V) in calcined, dehydrated CrAPSO-11. The identification of tetrahedral Cr(V) by both diffuse reflectance UV and by ESR suggests that the Cr(V) is indeed in a framework site.

The location of Cr(V) in a framework site is also strongly supported by the ^{31}P modulation data (Figure 9) which indicates 11−12 P nuclei surrounding Cr(V) at 0.58 nm. These parameters support Cr(V) substitution into a P(V) site for which, according to the SAPO-11 structure, there are 11 nearest P nuclei at 0.57 nm. These parameters exclude Cr(V) substitution into an Al site in SAPO-11 for which Cr(V) would have four nearest P nuclei at 0.31 nm. The ^{31}P parameters also seem inconsistent with an ion-exchange site. For example, Cr(V) in an ion-exchange site in the large channel coordinated to a six-ring would have three nearest P nuclei at <0.4 nm.

Note that in the synthesis procedure Cr(III) is present and is initially incorporated as Cr(III) into the SAPO-11 framework. There is good precedent based on pulsed ESR spectroscopic evidience that Cr(III) is likely to be incorporated into a P(V) framework site rather than into an Al(III) framework site. Previous spectroscopic evidence has shown that Ni(II) is incorporated into framework P(V) sites in NiAPSO-11,[38] NiAPSO-5,[39,40] and NiAPSO-41[41] rather than into Al(III) sites. As far as we are aware, the only evidence that metal ions incorporate into Al(III) sites rather than into P(V) sites in AlPO materials is based on bulk chemical analysis which is indirect at best.

Substitution of Cr(V) into a P(V) site in calcined CrAPSO-11 also seems consistent with the adsorbate geometry determined by ESEM. There is little difference in the adsorbate geometries for CrAPSO-11 versus (S)Cr−SAPO-11 except that the average distances are somewhat greater in (S)Cr−SAPO-11. In previous work with Ni(II)[38−41] substituting into P(V) sites in SAPO materials, the local site becomes negatively charged and the orientation of D_2O or CH_3OD dipolar molecules reflects this by adopting an H-bonded orientation. However, in calcined CrAPSO-11 Cr(V) substitution into a P(V) site causes no local charge change so that a dipole orientation of these dipolar molecules is found.

The TGA data also support Cr(III) substitution for P(V) rather than for Al(III) in as-synthesized CrAPSO-11 because new, stronger acid sites are indicated by the TGA data in CrAPSO-11 versus SAPO-11. Cr(III) substitution for Al(III) should not generate new acid sites because there is no charge change, while Cr(III) substitution for P(V) does generate new acid sites. This is indirect evidence for Cr(III) in as-synthesized CrAPSO-11 which is observed by ESR.

Additional indirect evidence for Cr(V) framework substitution in calcined CrAPSO-11 is provided by the slow kinetics for ND_3 or pyridine interaction with this Cr(V). This seems consistent with Cr(V) being in a framework position which exhibits less access to adsorbates than Cr(V) in an ion-exchange site. In contrast, the kinetics of ND_3 interaction with Cr(V) in (S)Cr−SAPO-11 are much faster (Figure 7).

Although the variety of the above evidence supports rather strongly that Cr(V) substitutes for framework P(V) in calcined CrAPSO-11, there are some unclear aspects. Although Cr(V) species 1 has been assigned to square-pyramidal Cr(V) based on a calculation of its ESR g parameters, the adsorbate coordination numbers of two for water, methanol, and ammonia do not seem consistent with this for Cr(V) in a tetrahedral framework site. These adsorbate numbers seem more consistent with distorted octahedral geometry, but that geometry predicts $g_\perp < g_\parallel$ which is not observed. Of course, it is known that calculations of ESR g parameters are not unambiguous. This point requires further study.

Overall, the data seem clear that the Cr(V) sites in (S)Cr−SAPO-11 and in calcined CrAPSO-11 are quite different. Furthermore, there is good evidence to support the assignment of Cr(V) in calcined CrAPSO-11 to a framework P(V) site.

Acknowledgment. This research was supported by the National Science Foundation and the Robert A. Welch Foundation. We thank Dr. M. Narayana for NMR measurements, Ms. L. Liu for TGA measurements, and Drs. A. M. Prakash and D. Zhao for helpful discussions.

References and Notes

(1) Lok, B. M.; Vail, L. D.; Flanigen, E. M. Eur. Patent Appl. E.P. 158, 348; 158, 975; 161, 491, 1985.

(2) Flanigen, E. M.; Lok, B. M.; Patton, R. L.; Wilson, S. T. Eur. Patent Appl. E.P. 158, 976, 1985; U.S. Patent 4, 759, 919; 4, 738, 837, 1988.

(3) Lok, B. M.; Marcus, B. K.; Flanigen, E. M. Eur. Patent Appl. E.P. 161, 490, 1985.

(4) Wilson, S. T.; Flanigen, E. M. U.S. Patent 4,567,029, 1986.

(5) Lok, B. M.; Messina, C. A.; Patton, R. L.; Gajek, R. T.; Cannan, T. R.; Flanigen, E. M. U.S. Patent 4,400,871, 1984.

(6) Chen, J. D.; Hans, E. B. L.; Roger, A. S. *J. Chem. Soc., Faraday Trans.* **1996**, *92*, 1806.

(7) Rajic, N.; Stojakovic, D.; Hocevar, S.; Kaucic, V. *Zeolites* **1993**, *13*, 384.

(8) Weckhuysen, B. M.; Schoonheydt, R. A. *Zeolites* **1994**, *14*, 360.

(9) Eswaramoorthy, M.; Jebarathinam, N. J.; Ulagappan, N.; Krishnasamy, V. *Catal. Lett.* **1996**, *38*, 255.

(10) Kornatowski, J.; Finger, G.; Jancke, K.; Richter-Mendan, J.; Schultze, D.; Joswig, W.; Baur, W. H. *J. Chem. Soc., Faraday Trans.* **1994**, *90*, 2141.

(11) Kevan, L. *Acc. Chem. Res.* **1987**, *20*, 1.

(12) Lee, C. W.; Chen, X.; Kevan, L. *J. Phys. Chem.* **1991**, *95*, 8626.

(13) Wilson, S. T.; Lok, B. M.; Flanigen, E. M. U.S. Patent 431,0440, 1982.

(14) Lee, C. W.; Chen, X.; Kevan, L. *J. Phys. Chem.* **1992**, *96*, 357.

(15) Lee, C. W.; Chen, X.; Kevan, L. *J. Phys. Chem.* **1992**, *96*, 3110.

(16) Kevan, L. In *Time Domain Electron Spin Resonance;* Kevan, L., Schwartz, R. N., Eds.; Wiley-Interscience: New York, 1979; Chapter 8.

(17) Dikanov, S. A.; Tsvetkov, Y. D. *Electron Spin Echo Envelope Modulation Spectroscopy*; CRC Press: Boca Raton, FL, 1992.

(18) Vedrine, J. C. In *Zeolite Chemistry and Catalysis;* Jacobs, P. A., Jaeger, N. I., Kubelkova, L., Wichterlova, B., Eds.; Elsevier: Amsterdam, 1991; p 25 [*Stud. Surf. Sci. Catal.* **1991**, *69*, 25].

(19) Garner, C. D.; Kendrick, J.; Lambert, P.; Mabbs, F. E.; Hillier, I. H. *Inorg. Chem.* **1976**, *15*, 1287.

(20) Simo, C.; Banks, E.; Holt, S. L. *Inorg. Chem.* **1970**, *9*, 183.

(21) Blackwell, C. S.; Patton, R. L. *J. Phys. Chem.* **1988**, *92*, 3965.

(22) Jahn, E.; Muller, D.; Becker, K. *Zeolites* **1990**, *10*, 151.

(23) Cornet, D.; Burwell, R. L. *J. Am. Chem. Soc.* **1968**, *90*, 2489.

(24) O'Reilly, D. E.; Maclver, D. S. *J. Phys. Chem.* **1962**, *66*, 276.

(25) Przheval'skaya, L. K.; Shvets, V. A.; Kazanskii, V. B. *Kinet. Catal.* **1970**, *11*, 1085.

(26) Weckhuysen, B. M.; Schoonheydt, R. A.; Mabbs, F. E.; Collison, D. *J. Chem. Soc., Faraday Trans.* **1996**, *92*, 2431.

(27) Howe, R. F. *J. Chem. Soc., Faraday Trans. 1* **1975**, *71*, 1689.

(28) Van Reijen, L. L.; Cossee, P. *Discuss. Faraday Soc.* **1966**, *41*, 277.

(29) Huang, M.; Deng, Z.; Wang, Q. *Zeolites* **1990**, *10*, 272.

(30) Kivelson, D.; Lee, S. K. *J. Chem. Phys.* **1964**, *41*, 1896.

(31) Aleksandrov, V.; Kazanskii, V. B.; Mikheikin, I. D. *Kinet. Catal.* **1965**, *6*, 383.

(32) McGarvey, B. R. *J. Phys. Chem.* **1967**, *71*, 51.

(33) Azuma, N.; Hartmann, M.; Kevan, L. *J. Phys. Chem.* **1995**, *99*, 6670.

(34) Huang, M.; Yao, J.; Xu, S.; Meng, C. *Zeolites* **1992**, *12*, 810.

(35) Przheval'skaya, L. K.; Shvets, V. A.; Kazanskii, V. B. *Kinet. Catal.* **1974**, *15*, 153.

(36) Kucherov, A. V.; Slinkin, A. A. *Zeolites* **1987**, *7*, 38.

(37) Azuma, N.; Lee, C. W.; Zamadics, M.; Kevan, L. In *Zeolite and Related Microporous Materials: State of the Art;* Weitkamp, J., Karge, H. G.;, Pfeifer, H., Holderich, W., Eds.; Elsevier: Amsterdam, 1994; p 805 [*Stud. Surf. Sci. Catal.* **1994**, *84*, 805].

(38) Azuma, N.; Lee, C. W.; Kevan, L. *J. Phys. Chem.* **1994**, *98*, 1217.

(39) Hartmann, M.; Azuma, N.; Kevan, L. *J. Phys. Chem.* **1995**, *99*, 10988.

(40) Hartmann, M.; Azuma, N.; Kevan, L. In *Zeolites: A Refined Tool for Designing Catalytic Sites;* Bonneviot, L., Kaliaguine, S., Eds.; Elsevier: New York, 1995; p 335 [*Stud. Surf. Sci. Catal.* **1995**, *97*, 335].

(41) Prakash, A. M.; Hartmann, M.; Kevan, L. *J. Chem. Soc., Faraday Trans.* **1997**, *93*, 1233.